Blockchain-enabled Carbon and Energy Trading for Network-Constrained Coal Mines with Uncertainties

Hongxu Huang, Zhengmao Li, *Member, IEEE*, L. P. Mohasha Isuru Sampath, Jiawei Yang, *Student Member, IEEE*, Hung D. Nguyen, Hoay Beng Gooi, *Fellow, IEEE*, Rui Liang, Dunwei Gong

***Abstract*—In this paper, a blockchain-enabled distributed market framework is proposed for the bi-level carbon and energy trading between coal mine integrated energy systems (CMIESs) and a virtual power plant (VPP) with network constraints. To maximize the profits of these two entities and describe their complicated interactions in the market, the bi-level trading problem is formulated as a Stackelberg game considering integrating the energy market and the "cap-and-trade" carbon market mechanism. Meanwhile, in the CMIES, energy recovery units and belt conveyors can be flexibly scheduled and the pumped hydroelectric storage in the VPP is scheduled for energy management. To tackle uncertainties from PV outputs, the joint trading, and the energy management is solved by the distributionally robust optimization (DRO) method. In addition, for participants' privacy, the alternating direction method of multipliers (ADMM) - based DRO algorithm is applied to solve the trading problem in a distributed framework. Further, the Proof-of-Authority (PoA) blockchain is deployed to develop a safe and anonymous market platform. Finally, case studies along with numerous comparison cases are conducted to verify the effectiveness of the proposed method. Simulation results indicate that the proposed method can effectively reduce the system operation cost and regional carbon emission, reduce the conservativeness and protect the privacy of each participant.**

***Index Terms*—Joint carbon and energy market, blockchain, distributionally robust optimization, ADMM**

NOMENCLATURE

A. Acronyms

ADMM	Alternating direction method of multipliers
BC	Belt conveyor
DSO	Distribution system operators
PHS	Pumped hydroelectric storage
TOU	Time-of-use tariff
VPP	Virtual power plant
CMIES	Coal mine integrated energy system

B. Indexes and Sets

$\mathcal{A}(n)$	Set of ancestor buses
$\mathcal{C}(n)$	Set of descendant buses
$\mathcal{N}/n$	Set/Index of buses in distribution grid
$\mathrm{N}_{\mathcal{I}}$	Set of CMIES
$\mathcal{H}/t$	Set/Indice of the operation time slots

C. Parameters

r_n/x_n	Resistance and reactance of the branch between the bus $\mathcal{A}(n)$ and n
α_i/β_i	Emission function parameters of CMIES i
η_d/η_m	Effciency parameter of the BC
$\lambda_{\mathrm{Grid}}^{\mathrm{S},t}/\lambda_{\mathrm{Grid}}^{\mathrm{B},t}$	Feed in/Purchase TOU tariff
V_{BC}	Belt speed of the BC
$\tau_{\mathrm{VPP}}^{\mathrm{S},t}/\tau_{\mathrm{VPP}}^{\mathrm{B},t}$	Sale/Purchase carbon emission right price of CMIES i from VPP
$\theta_1/\theta_2/\theta_3/\theta_4$	Design parameter of the BC
$a_i/b_i/c_i$	Cost function parameters of CMIES i
$\mathcal{T}_{ce}$	Carbon tax price

D. Variables

p_n/q_n	Active and reactive power injections of bus n
P_m/Q_m	Active/reactive power between bus n and $m \in \mathcal{C}(n)$
P_n/Q_n	Active/reactive power between bus $\mathcal{A}(n)$ and n
u_n	Voltage of bus n
$\kappa_{\mathrm{VPP}}^{\mathrm{S},t}/\kappa_{\mathrm{VPP}}^{\mathrm{B},t}$	Sale/Purchase power price of CMIES i from VPP
$ce_{\mathrm{VPP}}^{\mathrm{S},t}/ce_{\mathrm{VPP}}^{\mathrm{B},t}$	Sale/Purchase carbon emission right of CMIES i from VPP
$h_{\mathrm{TSTC}}^{i,t}/h_{\mathrm{TSTD}}^{i,t}$	Charging/Discharging thermal power of the TST in CMIES i at time t
$p_{\mathrm{CHP}}^{i,t}/p_{\mathrm{MT}}^{i,t}$	CHP/MT power output of CMIES i at time t
$p_{\mathrm{BC}}^{i,t}/q_{\mathrm{BC}}^{i,t}$	Power/Feed rate of the BC in CMIES i at time t
$p_{\mathrm{PHSC}}^{t}/p_{\mathrm{PHSD}}^{t}$	Charging/Discharging power of the PHS at time t
$\mathcal{CE}^i$	Carbon emission of CMIES i
$\mathcal{C}_i^{\mathrm{G}}$	Generation cost of CMIES i
$\mathrm{E}_{\mathrm{TST}}^{i,t+1}$	SOC of the TST in CMIES i at time t
$\mathrm{E}_{\mathrm{Silo},k}^{i,t}$	SOC of the kth Silo in CMIES i at time t
$\mathrm{E}_{\mathrm{PHS}}^{t}$	SOC of the PHS at time t
$ce_{\mathrm{L}}^{i,t}$	Carbon emission of CMIES i at time t

I. INTRODUCTION

THE coal mine industry is undergoing irreversible decarbonization with the clean energy supply and recovery. In coal mines, many energy resources such as ventilation air methane [1], coal seam gas [2] and gusing water [3] are recovered by means of power generation and exhaust heat recovery, which has enormous potential in the coal mine decarbonization.

Under this circumstance, the coordinated operation scheduling of CMIESs emerges to facilitate the synergies between electricity and thermal energy for economic benefits. In [4], CMIESs are equipped with various energy recovery units and deal with uncertainties by dispatching CMIESs under a two-stage robust stochastic optimization framework. To gain more profits, Ref. [5] considers the BCs and coal silos for demand response to save energy supply costs based on the time-of-use (TOU) tariff. Apart from the economic cost, multiple conflicting objectives of CMIESs are optimized with an piecewise NSGA II-based algorithm [6].

Meanwhile, as coal production gradually gets saturated in some coal seams, abandoned resources can be utilized for clean energy supply. Abandoned surface land resources are utilized for photovoltaic (PV) farms. Besides, PHS [7], a promising storage technology is also developed using the

abandoned goaf to charge and discharge at different times. Hence, by integrating PV generation with PHS dispatching management, a VPP can enhance the flexibility of renewable energy supply [8], [9].

Although in [4]–[6], the coordinated operational scheduling of CMIESs is studied, they are confined to a fixed TOU tariff. In fact, the total annual power demand of the coal mining process in China was 90.628 billion kWh in 2018 [10]. With such a huge demand, neglecting their dynamic pricing in an decentralized energy market will restrict the practicality and impair the welfares of coal mine enterprises. Meanwhile, in coal mines, the VPP and CMIESs are two kinds of entities connected to the same physical network. Typically, they have complex market roles depending on their power surplus or shortage. Nonetheless, previous studies have not reached how to balance their diverse and conflicting interests in a decentralized marketplace.

Given this insight, it is vital to design a suitable energy trading model with the leader–follower structure between the VPP and CMIESs for maximizing their own profits. Modelling their energy trading as a bi-level optimization problem [11], [12] is an effective approach to maximize their own benefits. In the marketplace, the VPP can take the leader position to give the price first and CMIESs follow the price to decide their commodity by the independent optimal scheduling. To deal with energy trading problems, cooperative [13]–[15] and non-cooperative game theories [16], [17] are widely studied. In these approaches, the Stackelberg game is well suited to describe the interaction between two parties with conflicting interests and/or a win-win optimal solution. In the literature, Ref. [18] addressed energy as a Stackelberg game with a bidding mechanism. The microgrid operator acts as the leader and all participating prosumers are considered as followers. Ref. [19] seeks to model the interaction between the retailer and consumers, and it is modeled as a one-leader-N-follower Stackelberg game. In [20], the coordination of demand response and internal prices in energy trading is considered in the Stackelberg game to present the consumers' behavior. Besides, the cost and utility models for prosumer benefits are established by modeling the energy trading between prosumers as a Stackelberg game. To further consider the trading strategies, in [21], the arbitrage strategy is enforced in the Stackelberg game where the equilibrium can both reduce the energy supply and carbon emission cost.

Although in [17]–[21], the energy trading is optimized to the game equilibrium, these studies only modelled the carbon emission as the penalty cost. Joint carbon and energy trading market has not been considered in these studies to obtain the Stackelberg equilibrium. According to the Kyoto Protocol, carbon trading markets [22] have been set in many countries and regions as the "cap-and-trade" market to reduce greenhouse gas emissions. Since the main carbon emission in energy system comes from fossil generation, how to integrate the carbon trading and energy trading as a joint marketplace is still a remaining issue.

Moreover, in the carbon and energy markets, the massive key private information, including energy price, power exchange quantity and units carbon emission parameters, should be protected to guarantee trading fairness. One effective privacy-preserving way is to solve the problem in a decentralized manner [23] as all the private information will be only kept within each party. In this regard, the ADMM, which deals with trading problems locally with a finite number of iterations and the guarantee of convergence, is appropriate [24]. In [25], the interaction between prosumers is addressed with the ADMM with their information updated in a decentralized manner. Ref. [26] deploys the ADMM method for the energy trading considering the voltage management in the distribution grid. However, these approaches are based on a third-party operator to manage the network, and can not preserve nodal information privacy. To the best of our knowledge, decentralized network operation and privacy preserved carbon and energy trading is still unaddressed in the literature.

Blockchain technology, as one of the promising distributed ledger technologies, has been studied for establishing a transparent and secure energy trading marketplace. Ref. [27] designs the consortium blockchain technology for a P2P electricity trading market among plug-in electric vehicles, which enables the aggregators to participate in a ensure privacy preserved and trustworthy P2P trading. Ref. [28] designs a hierarchical blockchain mechanism for the distributed control system operation and double auction mechanism-based energy trading. Ref. [29] establishes a neighboring energy marketplace for P2P energy trading, while a noise-based differential privacy algorithm is utilized to change the feature of transaction records without affecting the accuracy of records.

Nevertheless, these blockchain implementations are confined to auction-based trading mechanisms. Game theory, including the cooperative game, non-cooperative game and the Stackelberg game, can effectively capture complicated participants' interactions and strategies and achieve the game equilibrium. The cooperative game is applied to the multi microgrids to describe their energy trading behaviors under the blockchain base trading framework [30]. In [31], a non-cooperative game theory-based pricing model is proposed in a localized Practical Byzantine Fault Tolerance based-Consortium Blockchain (PBFT-CB) for the decentralized energy trading. The energy trading under the Stackelberg game framework in [32] is also processed by the credit-based blockchain to reduce the calculation cost and promote the exergy trading efficiency. However, these approaches execute the energy market clearing in a centralized manner, which cause the loss of data privacy and the efficiency of energy trading.

The distributed nature of blockchain framework enables the energy trading to be optimized by the distributed algorithm, which enhances the information privacy and computation efficiency. In [33], a decentralized energy trading algorithm is proposed to improve the individual benefit and guarantee the optimal performance of social welfare. The proposed algorithm matches the blockchain system to avoid privacy leakage in energy trading. To address the energy trading under the blockchain framework, the energy market is designed in [34] to be cleared by a decentralized Ant-Colony optimization method. Intertemporal energy trading is executed through smart contract implementation. Considering the dynamic net-

work operation and reconfiguration, the P2P energy trading is addressed with a decentralized optimization model which can adjust the network usage price to reach the balance between P2P electricity trading maximization and distribution network security [35]. However, to this end, the distribution network operation is not fully validated in the smart contract, which is vital for the practicality of energy trading.

From the research works above, it can be seen that though the ADMM method is applied in some research works, little attention has been paid to the privacy safety of the variable update process. Hence, a promising technology with pseudo-anonymous and immutability features called blockchain can be coordinated with the ADMM approach for better convergence performance and privacy-preserving. Nonetheless, how to develop a blockchain-enabled trading marketplace coordinating the distribution grid operation and energy trading is an challenging task in both academia and industry.

Last but not least, though various researches have been conducted on coal mines operation scheduling, the research on the joint carbon and energy market, decentralized trading under network operation and the blockchain-enabled privacy preservation has not been touched for the coal mine industry.

To address the research gaps identified above, this paper proposes a Stackelberg game-based joint carbon and energy trading framework for the VPP and CMIESs with optimal energy management. An ADMM-based DRO algorithm is proposed for a decentralized market-clearing while dealing with uncertainties from the renewables. Considering the privacy preservation, the PoA blockchain is deployed with the smart contract to protect key information and validate bus voltages. The main contributions of this work are summarized as:

1) A Stackelberg game-based carbon and energy trading marketplace is proposed for the VPP and CMIESs. From the eco-friendly energy policy perspective, a carbon allocation cap-based bi-level market is designed with non-cooperative energy market for regional decarbonization.
2) To tackle the uncertainties from PV outputs and solve the bi-level trading in a decentralized way, an ADMM-based DRO algorithm is proposed. The proposed approach effectively optimize the benefits of the VPP and CMIESs by coordinating the local energy management and their carbon and energy trading quantities.
3) A PoA blockchain is established to develop a safe and anonymous transaction platform. Key information updating, such as price and commodity, is encrypted in the smart contract. Information privacy can be fully guaranteed without sharing to a third-party.

II. Bi-level Trading Framework Under Network Management

The physical network architecture and the bi-level energy and carbon trading framework is presented in Fig. 1. Participants in the carbon and energy trading market are the VPP, the CMIESs, and the DSO. In the physical network, participants are highlighted with different colors. In the radial distribution grid, the ancestor node of VPP is connected to the DSO and the child node is connected to all the CMIESs. Each CMIES settles in different branches from the VPP. Their

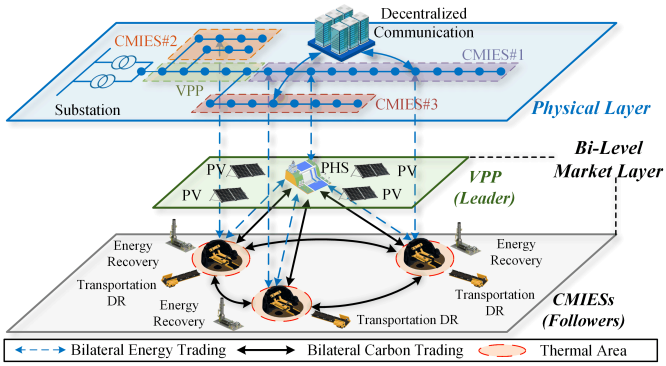

Fig. 1. Bi-level energy and carbon trading framework.

power exchange are coordinated to the network operation management in a decentralized manner.

1) VPP: With PV farms and the PHS system, the VPP can behave as a prosumer to sell and purchase power depending on its flexible energy management. Specifically, the power generation of VPP does not emit carbon dioxide, which enables the VPP to have excessive emission right to sell.

2) CMIES: Each CMIES is equipped with electrical and thermal energy recovery units. Besides, their coal transportation systems can be flexibly scheduled as demand response measures. With their energy management, the CMIESs are prosumers in the market.

3) DSO: The DSO is the electricity retailer that purchases or sells the electricity to the VPP and CMIESs when their energy supply is excessive or insufficient. It should be noted that the role of DSO is to keep the supply–demand balance in the distribution network with the fixed TOU tariff. As such, the DSO does not actively engage in the trading market. Energy transactions between the DSO and other entities are settled with a fixed TOU tariff.

A. Bi-level Carbon and Energy Trading Framework

1) Bi-level Trading Framework: Since the VPP and CMIESs have conflicting interests, a Stackelberg game can describe the bi-level decision process. In this study, the VPP integrates uncertain renewable energy supply and energy storage units, which can coordinate with all the CMIESs in the network. Thus, the VPP is modelled as the leader in the game that guides the energy transaction of CMIESs by using reasonable prices. Then the CMIESs, as the followers, have the liberty to decide the trading quantity or to trade with the DSO by the TOU tariff.

2) Carbon and Energy Market: With PV farms, the VPP can make a profit by selling excessive energy to the DSO or the CMIESs. The CMIESs can also have flexible energy transactions with either the VPP or the DSO based on their market quota. Energy transactions between the DSO and the VPP or the CMIESs are settled with a fixed TOU tariff. Typically, the power price given by the VPP should be within the range of the purchase and sale TOU tariffs given by the DSO. In case of power unbalance, the VPP and the CMIES will trade with the DSO, which brings fewer economic benefits to the VPP and CMIESs.

Required by the "cap-and-trade" mechanism, all the market participants are obligated to emit carbon dioxide within the

allocation and pay their own carbon emission tax. It is denoted that the energy supplied by VPP can be regarded as having no carbon emission. This empowers the VPP to gain trade profits by selling carbon emission rights without carbon tax cost. Thus, as mentioned in the bi-level framework, the VPP will firstly decide the price of carbon emission right as a leader. Then coal mine enterprises can purchase (sell) the emissions right from (to) others depending on its emission and its allocation cap.

Under the cap-and-trade mechanism, the VPP and CMIESs are firstly allocated some free emission rights from an authorized third party based on the grandfathering rule. The surplus or shortage of allocated emission rights can be traded by the participants as goods for economic benefits. It is worth denoting that the initial emission rights are regarded as parameters that can be adapted according to different cases. Hence, the proposed trading model can effectively achieve the game equilibrium without the loss of generality.

B. Distribution Network

To ensure that the energy transaction can be executed in the distribution grid, we utilize the linearized *Disflow* network model. In radial distribution grids $\mathcal{A}(1)=\emptyset$. The input buses of the CMIESs are denoted as $n\in\mathcal{I}(n)$ and the input bus of the VPP is denoted as $n\in\mathcal{J}(n)$, with $\mathcal{I}(n),\mathcal{J}(n)\subseteq\mathcal{N}$. The branch flow model for the distribution network is denoted as:

$$u_{\mathcal{A}(n)}=u_n+2r_nP_n+2x_nQ_n \tag{1a}$$

$$\underline{u}_n\le u_n\le\bar{u}_n \tag{1b}$$

$$P_n=\sum_{m\in\mathcal{C}(n)}P_m-p_n,\quad Q_n=\sum_{m\in\mathcal{C}(n)}Q_m-q_n \tag{1c}$$

For all bus $n\in\mathcal{N}$, Eq. (1a) constrains the voltage magnitude and the power flow by the *Ohm's Law*. Eq. (1b) denotes that the voltage magnitude of each bus should be within the range of maximal and minimal limits. Eq. (1c) enforces the active and reactive power balance in the distribution grid. Thus, the energy transaction should satisfy the distribution network constraints (1a)-(1c).

III. System Modelling and Problem Formulation

A. Optimization Model of the CMIESs

To reduce the economic cost, the CMIESs are to optimize their energy scheduling along with the energy and carbon trading according to the VPP decision by the following model.

1) Objective Function : The objective function of each CMIES $i\in\mathrm{N}_{\mathcal{I}}$ is formulated as:

$$\begin{aligned}\mathcal{O}^i_{\mathrm{CMIES}}=\sum_{t\in\mathcal{H}}\Bigg(&\mathcal{C}^{\mathrm{G}}_i\left(p^{i,t}_{\mathrm{CHP}},p^{i,t}_{\mathrm{MT}}\right)+\mathcal{T}_{ce}ce^{i,t}_{\mathrm{L}}\\&+\mathrm{C}^{\mathrm{OM}}_i(p^{i,t}_{\mathrm{FL}}+h^{i,t}_{\mathrm{TSTC}}+h^{i,t}_{\mathrm{TSTD}})\\&+\lambda^{\mathrm{B},t}_{\mathrm{Grid}}p^{\mathrm{B},t}_{\mathrm{Grid},i}\ -\lambda^{\mathrm{S},t}_{\mathrm{Grid}}p^{\mathrm{S},t}_{\mathrm{Grid},i}\\&+\kappa^{\mathrm{B},t}_{\mathrm{VPP},i}p^{\mathrm{B},t}_{\mathrm{VPP},i}-\kappa^{\mathrm{S},t}_{\mathrm{VPP},i}p^{\mathrm{S},t}_{\mathrm{VPP},i}\\&+\tau^{\mathrm{B}}_{\mathrm{VPP}}ce^{\mathrm{B},t}_{\mathrm{VPP},i}\ -\tau^{\mathrm{S}}_{\mathrm{VPP}}ce^{\mathrm{S},t}_{\mathrm{VPP},i}\Bigg)\end{aligned} \tag{2}$$

where $\mathcal{H}=\{0,1,2,\ldots\}$. $\mathcal{C}^{\mathrm{G}}_i\left(p^{i,t}_{\mathrm{CHP}},p^{i,t}_{\mathrm{MT}}\right)$ is the generation cost function of the CHP and MT, which will be denoted in (3). $\mathcal{T}_{ce}ce^{i,t}_{\mathrm{L}}$ is the carbon emission tax for the local carbon emission surplus $ce^{i,t}_{\mathrm{L}}$ with the fixed tax price $\mathcal{T}_{ce}$. The operation and maintenance units consists of the thermal storage tank and flexible loads, such as WSHP, ASHP and BCs, where the p. u. operation and maintenance cost is denoted as $\mathrm{C}^{\mathrm{OM}}_i$ with the flexible loads $p^{i,t}_{\mathrm{FL}}=p^{i,t}_{\mathrm{WSHP}}+p^{i,t}_{\mathrm{ASHP}}+p^{i,t}_{\mathrm{BC}}$. $h^{i,t}_{\mathrm{TSTC}}$ and $h^{i,t}_{\mathrm{TSTD}}$ are the thermal charging and discharging power of the thermal storage tank (TST). The third line in (2) denotes the energy trading between the DSO and the CMIESs with TOU tariff $\lambda^{\mathrm{B},t}_{\mathrm{Grid}}$ and $\lambda^{\mathrm{S},t}_{\mathrm{Grid}}$. Similarly, the energy trading cost from the VPP is denoted in the fourth line in (2) with the price $\kappa^{\mathrm{B},t}_{\mathrm{VPP},i}$ and $\kappa^{\mathrm{S},t}_{\mathrm{VPP},i}$ determined by the VPP and the commodities $p^{\mathrm{B},t}_{\mathrm{VPP},i}$ and $p^{\mathrm{S},t}_{\mathrm{VPP},i}$. For the carbon trading, $ce^{\mathrm{B},t}_{\mathrm{VPP},i}$ and $ce^{\mathrm{S},t}_{\mathrm{VPP},i}$ are the emission rights purchase (sale) from (to) the VPP respectively. $\tau^{\mathrm{B}}_{\mathrm{VPP}}$ and $\tau^{\mathrm{S}}_{\mathrm{VPP}}$ are the respective prices.

2) Cost Function: In the objective function in (2), the generation cost function of the CHP and the MT is given as follows:

$$\mathcal{C}^{\mathrm{G}}_i\left(p^{i,t}_{\mathrm{CHP}},p^{i,t}_{\mathrm{MT}}\right)=\sum_{X\in\{\mathrm{CHP,\ MT}\}}a_i(p^{i,t}_X)^2+b_ip^{i,t}_X+c_i \tag{3}$$

where $p^{i,t}_X$ represents for the power outputs of the CHP and MT.

3) Carbon Emission Function: Also, the local carbon emission surplus $ce^{i,t}_{\mathrm{L}}$ is determined by carbon emissions and emission right transactions in each CMIES, denoted as:

$$ce^{i,t}_{\mathrm{L}}=\mathcal{CE}_i\left(p^{i,t}_{\mathrm{CHP}},p^{i,t}_{\mathrm{MT}}\right)+ce^{\mathrm{S},t}_{\mathrm{VPP},i}-ce^{\mathrm{B},t}_{\mathrm{VPP},i} \tag{4a}$$

$$\mathcal{CE}_i\left(p^{i,t}_{\mathrm{CHP}},p^{i,t}_{\mathrm{MT}}\right)=\sum_{X\in\{\mathrm{CHP,\ MT}\}}\alpha_i\left(p^{i,t}_X\right)^2+\beta_ip^{i,t}_X \tag{4b}$$

Eq. (4a) represents for the carbon emission surplus in the i^{th} CMIES at the t^{th} hour. Eq. (4b) denotes the carbon emission from CHP and MT power generation respectively.

4) Units Operation Constraints: Power outputs of the CHP and MT are within the ramp up/down and thermal-electricity conversion constraints [36] as:

$$\underline{r}^i_X\le(p^{i,t+1}_X-p^{i,t}_X)\le\bar{r}^i_X;\ \forall X\in\{\mathrm{CHP,\ MT}\} \tag{5a}$$

$$h^{i,t}_X=p^{i,t}_X\eta^{\mathrm{HER},i}_X;\qquad\forall X\in\{\mathrm{CHP,\ MT}\} \tag{5b}$$

$$h^{i,t}_U=p^{i,t}_U\eta^{\mathrm{COP},i}_U;\qquad\forall U\in\{\mathrm{WSHP,\ ASHP}\} \tag{5c}$$

where $\underline{r}^i_X$ and $\bar{r}^i_X$ are the ramp up/down limits of the CHP and MT. $p^{i,t}_U$ represents for the power consumption of the WSHP and ASHP. $h^{i,t}_X$ and $h^{i,t}_U$ are the thermal outputs determined by the heat electricity ratio (HER) $\eta^{\mathrm{HER},i}_X$ and the coefficient of performance (COP) $\eta^{\mathrm{COP},i}_U$ respectively.

TSTs are deployed in the CMIESs for flexible thermal energy dispatching. The constraints of TSTs are given as:

$$\mathrm{E}^{i,t+1}_{\mathrm{TST}}=\mathrm{E}^{i,t}_{\mathrm{TST}}+\left(h^{i,t}_{\mathrm{TSTC}}-h^{i,t}_{\mathrm{TSTD}}\right)\Delta t \tag{6a}$$

$$\mathrm{E}^{i,0}_{\mathrm{TST}}=\mathrm{E}^{i,|\mathcal{H}|}_{\mathrm{TST}}=\mathrm{E}^{i,\mathrm{init}}_{\mathrm{TST}} \tag{6b}$$

$$\underline{\mathrm{E}}_{\mathrm{TST}}\le\mathrm{E}^{i,t}_{\mathrm{TST}}\le\bar{\mathrm{E}}_{\mathrm{TST}} \tag{6c}$$

$$\underline{h}^i_{\mathrm{TSTC}}\le h^{i,t}_{\mathrm{TSTC}}\le\bar{h}^i_{\mathrm{TSTC}} \tag{6d}$$

$$\underline{h}^i_{\mathrm{TSTD}}\le h^{i,t}_{\mathrm{TSTD}}\le\bar{h}^i_{\mathrm{TSTD}} \tag{6e}$$

Eq. (6a) denotes the characteristic of the thermal energy storage $\mathrm{E}_{\mathrm{TST}}^{i,t+1}$ with thermal energy charging and discharging. The stored thermal energy at the beginning and end of a day should be equal to the initial value, which is represented by (6b). The min/max variables constraints are in (6c)-(6e).

In coal mines, the BCs are the main coal transportation units to deliver raw coal from the work-face to the ground by consuming electricity. The energy consumption of coal transportation has a large proportion of the coal mine loads. Hence, with coal storage in the silos, the BCs have the potential for participating in demand response to reduce economic costs. Based on many well-known standards or specifications, such as ISO 5048, DIN 22101 and JISB 8805, a general BC energy consumption model [37] was proposed as:

$$\begin{aligned} p_{\mathrm{BC}}^{i,t} =& \frac{1}{\eta_d \eta_m}\left(\left(q_{\mathrm{BC}}^{i,t}\right)^2\left(\mathrm{V}_{\mathrm{BC}}\theta_1+\frac{1}{\mathrm{V}_{\mathrm{BC}}}\theta_3\right)\right. \\ &\left.+q_{\mathrm{BC}}^{i,t}\left(\frac{\mathrm{V}_{\mathrm{BC}}^2}{3.6}+\theta_4\right)+\mathrm{V}_{\mathrm{BC}}\theta_2\right) \end{aligned} \tag{7}$$

In this study, the optimal energy scheduling of the BCs is focused on its coal delivey, which is mainly affected by the feed rate. Coordinated with the coal silos, the coal transportation system can be scheduled for demand response under the coal delivery balance constraints. The virtual energy storage constraints are given as:

$$m_{\mathrm{BC},k}^{i,t} = \frac{q_{\mathrm{BC},k}^{i,t}}{3.6\times \mathrm{V}_{\mathrm{BC}}}, \quad m_{\mathrm{BC},1}^{i,t} = \mathrm{m}_{\mathrm{CF}}^{i,t} \tag{8a}$$

$$\mathrm{E}_{\mathrm{Silo},k}^{i,t+1} = \mathrm{E}_{\mathrm{Silo},k}^{i,t} + (m_{\mathrm{BC},k}^{i,t} - m_{\mathrm{BC},k+1}^{i,t})\Delta t \tag{8b}$$

$$\mathrm{E}_{\mathrm{Silo},k}^{i,0} = \mathrm{E}_{\mathrm{Silo},k}^{i,|\mathcal{H}|} = \mathrm{E}_{\mathrm{Silo},k}^{i,\mathrm{init}} \tag{8c}$$

$$\underline{\mathrm{E}}_{\mathrm{Silo},k}^{i} \le \mathrm{E}_{\mathrm{Silo},k}^{i,t} \le \bar{\mathrm{E}}_{\mathrm{Silo},k}^{i} \tag{8d}$$

Eq. (8a) represents the relationship between the coal delivery mass $m_{\mathrm{BC},k}^{i,t}$ and feed rate $q_{\mathrm{BC},k}^{i,t}$ of the kth level BC. Eq. (8b) shows the coal storage in the k^{th} level silo with k^{th} BC delivering coal into the silo and coal delivered out by the $k+1^{th}$ BC. Eq. (8c) ensures a sustainable transportation scheduling in each day. Besides, the coal delivery demand are also satisfied by delivering all the raw coal from the coal face to ground, which is ensured by (8c). Eq. (8d) denotes that coal storage of each silo should stay within its capacity limits.

Energy exchange and units operation variables are within the maximal and minimal constraints as:

$$\underline{\Theta}^{i,t} \le \Theta^{i,t} \le \bar{\Theta}^{i,t} \tag{9a}$$

where $\Theta^{i,t} = (p_{\mathrm{Grid},i}^{\mathrm{B},t}, p_{\mathrm{Grid},i}^{\mathrm{S},t}, p_{\mathrm{VPP},i}^{\mathrm{B},t}, p_{\mathrm{VPP},i}^{\mathrm{S},t}, ce_{\mathrm{VPP},i}^{\mathrm{B},t}, ce_{\mathrm{VPP},i}^{\mathrm{S},t}, p_{\mathrm{CHP}}^{i,t}, p_{\mathrm{MT}}^{i,t}, q_{\mathrm{CHP}}^{i,t}, q_{\mathrm{MT}}^{i,t}, p_{\mathrm{WSHP}}^{i,t}, p_{\mathrm{ASHP}}^{i,t}, m_{\mathrm{BC},k}^{i,t})$ is limited within the range between $[\underline{\Theta}^{i,t}, \bar{\Theta}^{i,t}]$.

5) Power and Thermal Energy Balances: For power balance in (1c), the active and reactive power injections $p_{n\in\mathcal{I}(n)}$ and $q_{n\in\mathcal{I}(n)}$ of bus $n \in \mathcal{I}(n)$ are given as:

$$\begin{aligned} p_{n\in\mathcal{I}(n)} =& p_{\mathrm{Grid},\mathcal{I}(1)}^{\mathrm{B},t} + p_{\mathrm{VPP},\mathcal{I}(1)}^{\mathrm{B},t} - p_{\mathrm{Grid},\mathcal{I}(1)}^{\mathrm{S},t} - p_{\mathrm{VPP},\mathcal{I}(1)}^{\mathrm{S},t} \\ &+ p_{\mathrm{CHP}}^{n,t} + p_{\mathrm{MT}}^{n,t} - p_{\mathrm{FL}}^{n,t} - p_{\mathrm{L}}^{n,t} \end{aligned} \tag{10a}$$

$$q_{n\in\mathcal{I}(n)} = q_{\mathrm{CHP}}^{n,t} + q_{\mathrm{MT}}^{n,t} - q_{\mathrm{FL}}^{n,t} - q_{\mathrm{L}}^{n,t} \tag{10b}$$

where the energy transaction commodity is only calculated at the intial bus $\mathcal{I}(1)$ of the ith CMIES. With (1c), the power balance of each CMIES can be validated for energy transactions in the distribution grid.

Thermal energy balance for each CMIES is ensured as:

$$h_{\mathrm{L}}^{i,t} = h_{\mathrm{CHP}}^{i,t} + h_{\mathrm{MT}}^{i,t} + h_{\mathrm{WSHP}}^{i,t} + h_{\mathrm{ASHP}}^{i,t} + h_{\mathrm{TSTD}}^{i,t} - h_{\mathrm{TSTC}}^{i,t} \tag{11}$$

B. Distributionally Robust Optimization Model of the VPP

As the leader in the Stackelberg game, the VPP is to make the first move by determining the price for energy transactions among the VPP and CMIESs. Uncertainties from the PV output are addressed by the DRO method.

1) Objective Function: The VPP with surplus PV generation and energy storage is to make more profits by minimizing the economic cost. In the day-ahead carbon and energy trading market, the transaction and energy management cost of the VPP can be formulated as:

$$\begin{aligned} \mathcal{O}_{\mathrm{VPP}} =& \sum_{t\in\mathcal{H}}\left(\mathrm{C}_{\mathrm{PHS}}^{\mathrm{OM}}(p_{\mathrm{PHSC}}^{t} + p_{\mathrm{PHSD}}^{t}) + \mathcal{T}_{ce}(ce_{\mathrm{L}}^{\mathrm{VPP},t})\right. \\ &+ \lambda_{\mathrm{Grid}}^{\mathrm{B},t} p_{\mathrm{Grid,VPP}}^{\mathrm{B},t} - \lambda_{\mathrm{Grid}}^{\mathrm{S},t} p_{\mathrm{Grid,VPP}}^{\mathrm{S},t} \\ &+ \sum_{i\in\mathrm{N}_{\mathcal{I}}}\left(\kappa_{\mathrm{VPP},i}^{\mathrm{S},t} p_{\mathrm{VPP},i}^{\mathrm{S},t} - \kappa_{\mathrm{VPP},i}^{\mathrm{B},t} p_{\mathrm{VPP},i}^{\mathrm{B},t}\right) \\ &\left.+ \sum_{i\in\mathrm{N}_{\mathcal{I}}}\left(\tau_{\mathrm{VPP}}^{\mathrm{S}} ce_{\mathrm{VPP},i}^{\mathrm{S},t} - \tau_{\mathrm{VPP}}^{\mathrm{B}} ce_{\mathrm{VPP},i}^{\mathrm{B},t}\right)\right) \end{aligned} \tag{12}$$

The first part $\mathrm{C}_{\mathrm{PHS}}^{\mathrm{OM}}(p_{\mathrm{PHSC}}^{t} + p_{\mathrm{PHSD}}^{t})$ in the objective function (12) is the operation maintenance cost of the PHS. $\mathcal{T}_{ce}(ce_{\mathrm{VPP}}^{\mathrm{L},t})$ is the carbon emission tax cost for the local emission surplus $ce_{\mathrm{VPP}}^{\mathrm{L},t}$. $\left(\lambda_{\mathrm{Grid}}^{\mathrm{B},t}\right)^{\mathrm{T}} p_{\mathrm{Grid,VPP}}^{\mathrm{B},t} - \left(\lambda_{\mathrm{Grid}}^{\mathrm{S},t}\right)^{\mathrm{T}} p_{\mathrm{Grid,VPP}}^{\mathrm{S},t}$ denotes the cost of energy exchange between the VPP and the DSO with fixed purchase and sale price $\lambda_{\mathrm{Grid}}^{\mathrm{B},t}$ and $\lambda_{\mathrm{Grid}}^{\mathrm{S},t}$ respectively. For the energy exchange among the VPP and all the CMIESs $i \in \mathrm{N}_{\mathcal{I}}$, the cost of the VPP is denoted as $\sum_{i\in\mathrm{N}_{\mathcal{I}}}\left(\kappa_{\mathrm{VPP},i}^{\mathrm{S},t}\right)^{\mathrm{T}} p_{\mathrm{VPP},i}^{\mathrm{S},t} - \left(\kappa_{\mathrm{VPP},i}^{\mathrm{B},t}\right)^{\mathrm{T}} p_{\mathrm{VPP},i}^{\mathrm{B},t}$ where $\kappa_{\mathrm{VPP},i}^{\mathrm{B},t}$ and $\kappa_{\mathrm{VPP},i}^{\mathrm{S},t}$ are the energy purchase and sale price for CMIESs respectively. $p_{\mathrm{VPP},i}^{\mathrm{B},t}$ and $p_{\mathrm{VPP},i}^{\mathrm{S},t}$ are the purchase and sale commodities respectively, which are determined by the CMIESs as the followers. For the carbon emission right transaction, the corresponding cost is formulated as $\sum_{i\in\mathrm{N}_{\mathcal{I}}}\left(\tau_{\mathrm{VPP}}^{\mathrm{S}}\right)^{\mathrm{T}} ce_{\mathrm{VPP},i}^{\mathrm{S},t} - \left(\tau_{\mathrm{VPP}}^{\mathrm{B}}\right)^{\mathrm{T}} ce_{\mathrm{VPP},i}^{\mathrm{B},t}$ with fixed prices $\tau_{\mathrm{VPP}}^{\mathrm{S}}$ and $\tau_{\mathrm{VPP}}^{\mathrm{B}}$ and emission right commodities $ce_{\mathrm{VPP},i}^{\mathrm{S},t}$ and $ce_{\mathrm{VPP},i}^{\mathrm{B},t}$.

2) Pricing Criteria: For energy transactions, the clearing price for the CMIESs and power commodity from the DSO are within the maximal and minimal ranges denoted as follows:

$$\lambda_{\mathrm{Grid}}^{\mathrm{S},t} \le \kappa_{\mathrm{VPP},i}^{\mathrm{B},t} \le \lambda_{\mathrm{Grid}}^{\mathrm{B},t},\ 0 \le p_{\mathrm{Grid,VPP}}^{\mathrm{B},t} \le \bar{p}_{\mathrm{Grid,VPP}}^{\mathrm{B}} \tag{13a}$$

$$\lambda_{\mathrm{Grid}}^{\mathrm{S},t} \le \kappa_{\mathrm{VPP},i}^{\mathrm{S},t} \le \lambda_{\mathrm{Grid}}^{\mathrm{B},t},\ 0 \le p_{\mathrm{Grid,VPP}}^{\mathrm{S},t} \le \bar{p}_{\mathrm{Grid,VPP}}^{\mathrm{S}} \tag{13b}$$

3) Energy Storage Unit: Apart from energy transactions, the energy management of the energy storage unit is under the constraints [4] as:

$$\mathrm{E}_{\mathrm{PHS}}^{t+1} = \mathrm{E}_{\mathrm{PHS}}^{t} + \left(p_{\mathrm{PHSC}}^{t} - p_{\mathrm{PHSD}}^{t}\right)\Delta t \tag{14a}$$

$$\mathrm{E}_{\mathrm{PHS}}^{0} = \mathrm{E}_{\mathrm{PHS}}^{|\mathcal{H}|} = \mathrm{E}_{\mathrm{PHS}}^{\mathrm{init}} \tag{14b}$$

$$\underline{\mathrm{E}}_{\mathrm{PHS}} \le \mathrm{E}_{\mathrm{PHS}}^{t} \le \bar{\mathrm{E}}_{\mathrm{PHS}} \tag{14c}$$

$$\underline{p}_{\mathrm{PHSC}} \leq p^{t}_{\mathrm{PHSC}} \leq \bar{p}_{\mathrm{PHSC}} \tag{14d}$$

$$\underline{p}_{\mathrm{PHSD}} \leq p^{t}_{\mathrm{PHSD}} \leq \bar{p}_{\mathrm{PHSD}} \tag{14e}$$

4) Power Balance: For power balance in (1c), the active and reactive power injections of bus $n \in \mathcal{J}(n)$ is given as:

$$\begin{aligned} p_{n\in\mathcal{J}(n)} = & p^{\mathrm{B},t}_{\mathrm{Grid},\mathcal{J}(1)} + p^{\mathrm{B},t}_{\mathcal{J}(n),i} - p^{\mathrm{S},t}_{\mathrm{Grid},\mathcal{J}(1)} - p^{\mathrm{S},t}_{\mathcal{J}(n),i} \\ & + \tilde{p}^{n,t}_{\mathrm{PV}} + p^{n,t}_{\mathrm{PHSD}} - p^{n,t}_{\mathrm{PHSC}} - p^{n,t}_{\mathrm{L}} \end{aligned} \tag{15a}$$

$$q_{n\in\mathcal{J}(n)} = -q^{n,t}_{\mathrm{L}} \tag{15b}$$

where $\tilde{p}^{n,t}_{\mathrm{PV}}$ is the uncertain PV output.

5) Cap-and-trade Carbon Trading Mechanism : The carbon emission right trading is under the regional carbon emission allocation constraint as:

$$\sum_{i}^{\mathrm{N}_i} \left(ce^{\mathrm{B},t}_{\mathrm{VPP},i} - ce^{\mathrm{S},t}_{\mathrm{VPP},i} \right) = ce^{\mathrm{VPP},t}_{\mathrm{L}} \tag{16a}$$

$$\sum_{t}^{\mathrm{T}} \left(ce^{\mathrm{VPP},t}_{\mathrm{L}} + \sum_{i}^{\mathrm{N}_{\mathcal{I}}} ce^{i,t}_{\mathrm{L}} \right) \leq \bar{\mathrm{ce}}^{\mathrm{Cap}} \tag{16b}$$

$$\sum_{t}^{\mathrm{T}} \sum_{i}^{\mathrm{N}_i} \left(ce^{\mathrm{B},t}_{\mathrm{VPP},i} - ce^{\mathrm{S},t}_{\mathrm{VPP},i} \right) = 0 \tag{16c}$$

where $\mathrm{N}_{\mathcal{I}}$ is the number of CMIESs and $\bar{\mathrm{ce}}^{\mathrm{Cap}}$ is the regional carbon emission limit pre-allocated by a concerned third party, such as the cap-and-trade system in many countries. It is worth noting that the carbon trading market framework can be adapted to a peer centric trading framework among all the CMIESs by ensuring the VPP's carbon right trading surplus is zero over all time intervals, which is denoted in Eq. (16c).

6) Uncertainty Modelling: In this study, we consider a scenario based ambiguity set for modelling the uncertain PV output in the DRO. First, we define that the random variable $\hat{w} = \tilde{p}^{n,t}_{\mathrm{PV}} / \hat{p}^{n,t}_{\mathrm{PV}}$ as uncertain PV output over the forecasted value. In the DRO framework, we consider the Wasserstein metric [38] to constrain the uncertain variable $\tilde{w}$ centered around the distribution $\hat{\mathbb{P}}$. The Wasserstein metric is denoted as a tractable distance $\rho_{\mathrm{w}} : \mathbb{R}^{I_w} \times \mathbb{R}^{I_w}$ by the following equation:

$$\begin{aligned} d_{\mathrm{W}}(\mathbb{P}, \widehat{\mathbb{P}}) & \inf_{\mathbb{Q}\in\mathcal{Q}(\mathbb{P},\widehat{\mathbb{P}})} \mathbb{E}_{\mathbb{Q}}[\rho_{\mathrm{w}}(\tilde{w}, \hat{w})] \\ & = \left(\inf_{\mathbb{Q}\in\mathcal{Q}(\mathbb{P},\widehat{\mathbb{P}})} \int_{\mathbb{R}^{I}w \times \mathbb{R}^{I}w} \rho_{\mathrm{w}}(\tilde{w}, \hat{w})^2 \mathbb{Q}(d\tilde{w}, d\hat{w}) \right)^{1/2} \end{aligned} \tag{17}$$

where $\tilde{w} \sim \mathbb{P}$, $\hat{w} \sim \hat{\mathbb{P}}$ and $\mathcal{Q}(\mathbb{P}, \hat{\mathbb{P}})$ is the set of all joint probability distributions on $\mathbb{R}^{I_w} \times \mathbb{R}^{I_w}$ with marginals $\mathbb{P}$ and $\hat{\mathbb{P}}$. To ease the burden of computation, one natural approach to describe the PV output based on different scenarios $s \in S$ is to use the uniform distribution $\hat{\mathbb{P}}$ on the discrete scenario set S. Hence, $\hat{\mathbb{P}} = \frac{1}{S} \sum_{s\in[S]} \delta_{\tilde{w}_s}$. Then the Wasserstein ambiguty set is formulated by limiting the Wasserstein metric $d_{\mathrm{W}}(\mathbb{P}, \widehat{\mathbb{P}})$ less than the radius θ. The radius θ of the Wasserstein metric can be adjusted to adapt to the robustness requirement of the uncertainties. Then, to formulate the Wassersteim ambiguity set as a scenario-wise one, the auxiliary variable, $\tilde{v}$, is introduced for constraining the range of distance, $\rho_{\mathrm{w}}(\tilde{w}, \hat{w})$. For different scenarios $s \in S$, the primary random variable $\tilde{w}$ and the auxiliary random variable $\tilde{v}$ jointly formulate the support sets $\mathcal{Z}_s = \{(\tilde{w}, \tilde{v}) \mid \rho_{\mathrm{w}}(\tilde{w}, \hat{w}) \leq \tilde{v}, \hat{w} \sim \hat{\mathbb{P}}\}$ in the $\mathcal{F}_{\mathrm{w}}(\theta)$. Then the Wasserstein ambiguity set is denoted as Eq.(18). One tractable approach to solve the DRO problem with the Wasserstein ambiguity set is known as linear decision rule approach [39].

$$\mathcal{F}_{\mathrm{w}}(\theta) = \left\{ \mathbb{P} \in \mathcal{P}_0 \;\middle|\; \begin{array}{l} ((\tilde{w}, \tilde{v}), \tilde{s}) \in \mathbb{P} \\ \mathbb{E}_{\mathbb{P}}[\tilde{v} \mid \tilde{s} \in [S]] \leq \theta \\ \mathbb{P}\left[(\tilde{w}, \tilde{v}) \in \mathcal{Z}_s | \tilde{s} = s\right] = 1, \; \forall s \in [S] \\ \mathbb{P}[\tilde{s} = s] = \frac{1}{s}, \qquad \forall s \in [S] \end{array} \right\} \tag{18}$$

C. Bi-Level Optimization Reformulation

We formulate the bi-level optimization problem of the VPP and the CMIESs according to their the leader and follower position in the Stackelberg game. We formulate the bi-level optimization problem as follows.

1) Upper Level Problem Reformulation: To this end, the upper level problem of the VPP is reformulated as:

$$\min_{\mathbf{x}} \sup_{\mathbb{P}\in\mathcal{F}_{\mathrm{w}}(\theta)} \mathbb{E}_{\mathbb{P}} \, \mathcal{O}_{\mathrm{VPP}} + \frac{\rho}{2} \left\| \mathbf{x} - \hat{\mathbf{x}} \right\|_2^2 \tag{19a}$$

$$\text{s.t. } (1),(13)\text{-}(16),(18) \tag{19b}$$

where the objective is in the expected sense of total trading and operation cost with the uncertain PV output in the $\mathcal{F}_{\mathrm{w}}(\theta)$. Decision variables in the VPP is denoted as $\mathbf{x} = \Big[\kappa^{\mathrm{B},t}_{\mathrm{VPP},i}, \kappa^{\mathrm{S},t}_{\mathrm{VPP},i}, ce^{\mathrm{B},t}_{\mathrm{VPP},i}, ce^{\mathrm{S},t}_{\mathrm{VPP},i}, p^{\mathrm{B},t}_{\mathrm{Grid,VPP}}, p^{\mathrm{S},t}_{\mathrm{Grid,VPP}}, p^{t}_{\mathrm{PHSC}}, p^{t}_{\mathrm{PHSD}} \Big]$. The second part in the objective function is the quadratic penalty terms that augment the optimal solution towards the Stackelberg equilibrium. $\hat{\mathbf{x}}$ are the pre-solved decision results in the last iteration and ρ is the step size parameter used in the ADMM.

2) Lower Level Problem Reformulation: After the solution of the upper level problem, the CMIESs is to optimize its trading and the energy management problem is formulated as:

$$\min_{\mathbf{z}} \mathcal{O}^{\mathrm{i}}_{\mathrm{CMIES}} + \frac{\rho}{2} \left\| \mathbf{z} - \hat{\mathbf{z}} \right\|_2^2 \tag{20a}$$

$$\text{s.t. } (1),(3)\text{-}(11) \tag{20b}$$

where the decision variables $\mathbf{z}$ of the CMIESs are denoted as $\mathbf{z} = \big[p^{\mathrm{B},t}_{\mathrm{Grid},i}, p^{\mathrm{S},t}_{\mathrm{Grid},i}, p^{\mathrm{B},t}_{\mathrm{VPP},i}, p^{\mathrm{B},t}_{\mathrm{VPP},i}, p^{i,t}_{\mathrm{CHP}}, p^{i,t}_{\mathrm{MT}}, p^{i,t}_{\mathrm{WSHP}}, p^{i,t}_{\mathrm{BC}}, p^{i,t}_{\mathrm{ASHP}}, q^{i,t}_{\mathrm{CHP}}, q^{i,t}_{\mathrm{MT}}, q^{i,t}_{\mathrm{WSHP}}, q^{i,t}_{\mathrm{ASHP}}, q^{i,t}_{\mathrm{BC}}, h^{i,t}_{\mathrm{TSTC}}, h^{i,t}_{\mathrm{TSTD}} \big]$. Similarly, $\hat{\mathbf{z}}$ are the decision results in the last iteration. ρ is the step size parameter used for augmenting the optimal solution with the quadratic penalty terms of $\mathbf{z}$ in the ADMM.

IV. Stackelberg Game-based Market Coordination and Optimization Algorithm

A. Proof of Stackelberg Equilibrium

In this study, the transaction between the VPP and the CMIESs is formulated as the one leader multiple followers Stackelberg game. As the leader, the VPP announces the energy price $\kappa^{\mathrm{B/S}}_{\mathrm{VPP},i}$ first. The CMIESs, as followers, follow the price decision by announcing their willingness for energy exchange. All the leader and followers are to minimize their own cost respectively and reach the optimal strategies for all the participants. This is the Stackelberg equilibrium.

Considering a game Ξ played by the VPP j and the CMIESs $i \in \mathrm{N}_{\mathcal{I}}$, this game is formulated as:

$$\Xi = \left\{ (j \cup \mathrm{N}_{\mathcal{I}}), \{\kappa^{\mathrm{B/S}}_{\mathrm{VPP},i}\}_j, \{p^{\mathrm{B/S}}_{\mathrm{VPP},i}\}_{i\in \mathrm{N}_{\mathcal{I}}}, O^{\mathrm{VPP}}, \{O^i\}_{i\in \mathrm{N}_{\mathcal{I}}} \right\} \tag{21}$$

where $\{\kappa^{\mathrm{B/S}}_{\mathrm{VPP},i}\}_j$ is the set of purchase and sale pricing strategies of the VPP. $\{p^{\mathrm{B/S}}_{\mathrm{VPP},i}\}_{i\in \mathrm{N}_{\mathcal{I}}}$ is the set of power exchange strategies of the CMIESs. O^{VPP} and $\{O^i\}_{i\in \mathrm{N}_{\mathcal{I}}}$ are the objective functions of the VPP and the CMIESs respectively. Then, the Stackelberg equilibrium is defined as:

Definition 1. *Considering the game Ξ in (21), a set of strategies $(\kappa^{\star\mathrm{B/S}}_{\mathrm{VPP},i}, p^{\star\mathrm{B/S}}_{\mathrm{VPP},i})$ attains the equilibrium if and only if the following conditions are satisfied:*

$$\begin{aligned} &O^{\mathrm{VPP}}(\kappa^{\star\mathrm{B/S}}_{\mathrm{VPP},i}, p^{\star\mathrm{B/S}}_{\mathrm{VPP},i}) \le O^{\mathrm{VPP}}(\kappa^{\star\mathrm{B/S}}_{\mathrm{VPP},i}, p^{\mathrm{B/S}}_{\mathrm{VPP},i}), \\ &O^{i}(\kappa^{\star\mathrm{B/S}}_{\mathrm{VPP},i}, p^{\star\mathrm{B/S}}_{\mathrm{VPP},i}) \le O^{i}(\kappa^{\mathrm{B/S}}_{\mathrm{VPP},i}, p^{\star\mathrm{B/S}}_{\mathrm{VPP},i});\ \forall i \in \mathrm{N}_{\mathcal{I}} \end{aligned} \tag{22}$$

Once the equilibrium got attained, no other strategies can bring more benefits for any participants in the game. Then we can get Theorem 1 to prove the existence and uniqueness of the Stackelberg equilibrium in the game Ξ.

Theorem 1. *The Stackelberg equilibrium $(\kappa^{\star\mathrm{B/S}}_{\mathrm{VPP},i}, p^{\star\mathrm{B/S}}_{\mathrm{VPP},i})$ exists and is unique in the Stackelberg game Ξ.*

Proof. The objective function in Eq. (19a) and Eq. (20a) are continuous and differentiable. Then the Hessian matrices with their own strategies $(\kappa^{\mathrm{B}}_{\mathrm{VPP},i}, \kappa^{\mathrm{S}}_{\mathrm{VPP},i})$ and $(p^{\mathrm{B}}_{\mathrm{VPP},i}, p^{\mathrm{S}}_{\mathrm{VPP},i})$ are:

$$H_{\mathrm{VPP}}/H_i = \begin{bmatrix} \rho & 0 \\ 0 & \rho \end{bmatrix} \tag{23}$$

Since ρ is a positive constant, the Hessian matrices are all positive definite with their own strategies. This means that the conditions of equilibrium are satisfied. We have the following equation:

$$\begin{aligned} (\kappa^{\star\mathrm{B/S}}_{\mathrm{VPP},i}, p^{\star\mathrm{B/S}}_{\mathrm{VPP},i}) = \arg\min(O^{\mathrm{VPP}}, \{O^i\}_{i\in \mathrm{N}_{\mathcal{I}}}), \\ \forall (\kappa^{\mathrm{B/S}}_{\mathrm{VPP},i}, p^{\mathrm{B/S}}_{\mathrm{VPP},i}) \in \Xi \end{aligned} \tag{24}$$

Hence, the Theorem 1 is proved. □

B. Distributed Market Clearing Algorithm

Although the problem is strictly convex and can be solved in a centralized manner, e.g., by the VPP, there are still some drawbacks. Firstly, the CMIESs are not willing to share their private information, such as the energy exchange and carbon emission parameters in (4b); Also, a centralized solving approach will burden the computational inefficiency and latency, which is related to the number of scenarios in the DRO. Besides, each participant only knows partial information of the power flow variables in (1a)-(1c), (10a)-(10b) and (15a)-(15b). Sharing their power flow information can be beneficial to decentralized voltage management in the distribution grid.

To coordinate the VPP and the CMIESs in the bi-level DRO problem in a decentralized way, one approach is to use the decentralized feature of the ADMM algorithm. Since we have proved the *strictly convexity* of the proposed problem in Theorem 1, and the optimization problems (20) and (21) consist of *convex* inequality and *affine* equality constraints. This feature satisfies the *Slater's condition*, which indicates that the duality gap is zero in the proposed optimization problem. Thus, the convergence condition of the ADMM-based algorithms are satisfied and the detailed proof of the convergence and global optimality is studied in [24]. To validate the execution of the energy trading without violating the distribution grid model in (1a)-(1c), we consider the node voltage u and the residual r^k [24] by the abstract power flow constraints as:

$$u^{k+1} = u^k + A\mathbf{x}^k + B\mathbf{z}^k - c \tag{25}$$

$$r^{k+1} = \left\|\mathbf{x}^k - \mathbf{x}^{k-1}\right\|_2^2 + \left\|\mathbf{z}^k - \mathbf{z}^{k-1}\right\|_2^2 + \left\|u^k - u^{k-1}\right\|_2^2 \tag{26}$$

where k is the iteration in the ADMM. Considering the DRO problem, the pseudo-code distributed market coordination and optimization algorithm is illustrated in Algorithm 1.

Algorithm 1: ADMM-based Market Clearing

Input : $\lambda^{\mathrm{B},t}_{\mathrm{Grid}}, \lambda^{\mathrm{S},t}_{\mathrm{Grid}}, \tau^{\mathrm{B}}_{\mathrm{VPP}}, \mathcal{T}_{ce}, \tau^{\mathrm{S}}_{\mathrm{VPP}}, \hat{p}^{n,t}_{\mathrm{PV}}, \mathbf{x}^{(0)}, \mathbf{z}^{(0)}$
$\rho, \theta, \epsilon, k = 1, r^1 = +\infty$

while $r^k \ge \epsilon$ **do**
  Receive $\mathbf{z}^{k-1}$, Solve the DRO problem (19a).
  Broadcast $\mathbf{x}^{(k)}$ to the CMIESs: *x-update*
  Receive $\mathbf{x}^k$, Solve the problem (20a).
  Broadcast $\mathbf{z}^{(k)}$ to the VPPs: *z-update*
  Calculate the voltage residual (25).
  Broadcast $u^{(k)}$ to all bus node: *u-update*.
  $k \leftarrow k + 1$
end

Output: $\mathbf{x}^k, \mathbf{z}^k, u^k$

C. Implementation of the PoA Blockchain

To provide a privacy-preserving environment for the execution of the ADMM-based DRO algorihtm, we set up the PoA private blockchain on the Ethereum platform. The implementation of the PoA blockchain is shown in Fig. 2.

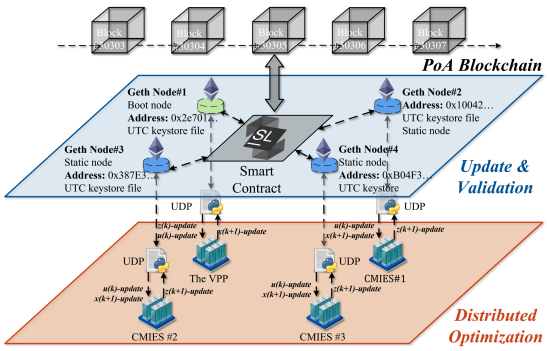

Fig. 2. The implementation of the PoA blockchain with ADMM update.

In the optimization layer, after the local decision of the VPP and the CMIESs, the *x-update*, *y-update* and *u-update* process data are sent to the User Datagram Protocol (UDP), which will transfer the updated variables to the Ethereum client *Geth*. We create a private blockchain network using the PoA protocol in Geth. The smart contract which is designed for variables update and voltage validation, is self-executed within

Algorithm 2: Smart contract with voltage validation

for each $Block(b_n)$ **do**
  Require $node.engage = true$
  Receive data from the UDP.
  Receive data from the $Block(b_{n-1})$.
  Calculate the residual $r^{(b_n)}$
  if $r^{(b_n)} < \epsilon$ **then**
    if $u^{(b_n)} \in [\underline{u}, \bar{u}]$ **then**
      Broadcast the transaction to Geth nodes;
    else
      Reject the transaction;
    end
  end
  Broadcast $\mathbf{x}^{(b_n)}, \mathbf{z}^{(b_n)}$ and $u^{(b_n)}$ to all nodes;
  Return data via UDP;
end

the blockchain network. The data in the blocks generated are encrypted by the ***Hash-function*** which is almost irreversible to be decoded. In Block(b_n), the information broadcast is encrypted by the ***Hash-function*** and passed down to the next Block(b_{n+1}), which can be denoted as:

$$Block(b_{n+1}) = Hash(\mathbf{x}, \mathbf{z}, u, t, Block(b_n), \text{SC}) \quad (27)$$

where b_n is the sequence of the blocks and SC represents the smart contract that is shown in Algorithm 2. Local optimization solutions are updated for all Geth nodes and be broadcasted to the participants following the PoA protocol. Thus, the variable update processes in the smart contract will continue until the stopping criterion of Algorithm 1 is satisfied. Then, the smart contract will validate the bus voltages to obtain an executable transaction, which ensures the security of the distribution grid.

The PoA blockchain is set up on the Ethereum platform. Each blockchain node is assigned with a private key and an address. The communication network is set up via the bootnode tool which is a service of the private PoA blockchain, which is more secure and efficient for decentralized energy trading.

V. Case Studies

The proposed bi-level energy and carbon trading with DRO energy management is tested on the IEEE 33-bus test system for the coal mine distribution grid to illustrate the effectiveness. The system configuration of the test coal mines is the same in Fig. 3. Fig. 4 represents the 50 uncertain scenarios of the PV output. The carbon tax price $\mathcal{T}_{ce}$ is set to $\$5.5$/ton and the purchase (sale) carbon emission right price is set as $\$6.5$ (4.5)/ton. The mathematical models are solved on a MATLAB 2021b platform with the commercial solver Gurobi 9.1.2 [40]. The relative gap is set at 10^{-5}. Parameters for different energy units and loads are listed in Table I.

A. Energy trading and management results of the VPP

Fig. 5 represents the energy price with the comparison of the TOU tariff and Fig. 6 shows the energy exchange between the VPP and the CMIESs respectively.

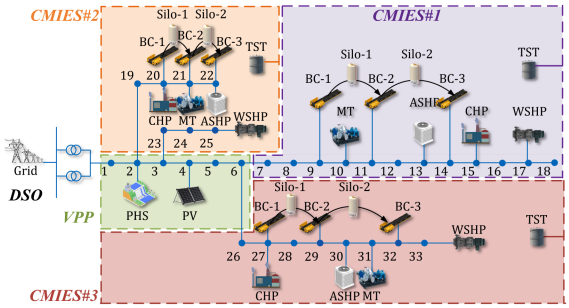

Fig. 3. System configuration for case study.

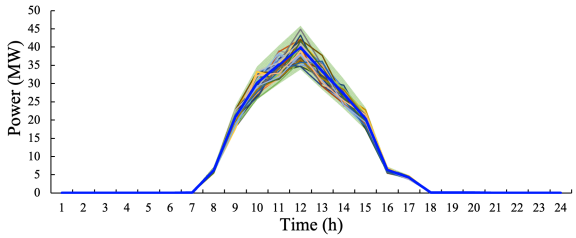

Fig. 4. Uncertain PV output Scenarios.

TABLE I
Technical Parameters of Energy Units

Units	Rated Power/ Capacity	Min/Max Ramp Power	Units	Rated Power/ Capacity	Min/Max Ramp Power
PV	60 MW/-	-	WSHP	0.8 MW/-	-0.2/0.2 MW
PHS	10 MW/80 MWh	-8/8 MW	ASHP	0.4 MW/-	-0.2/0.2 MW
CHP	25&50 MW/-	-8/8 MW	TST	10 MW/40 MWh	-4/4 MW
MT	25&50 MW/-	-25/25 MW			

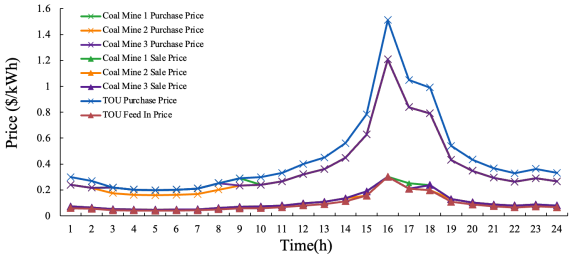

Fig. 5. Comparison of the energy trading price and the TOU tariff.

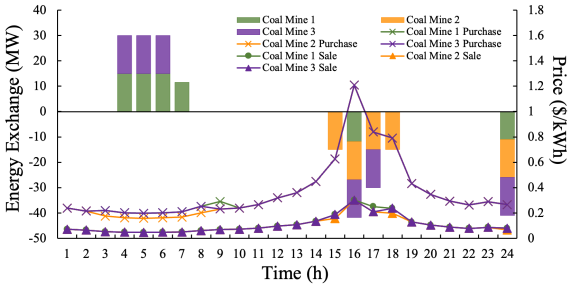

Fig. 6. Energy exchange between the VPP and the CMIESs.

Fig. 5 shows that the energy price is within the range of the purchase and sale TOU tariff. During the low-price time slots, such as 4:00-7:00, the power purchase price for the CMIESs is relatively high. Also, during high-price time slots, such as 15:00-18:00, the power purchase price is relatively lower than the TOU tariff. They should be considered with the energy exchange quantity results. Fig. 6 shows the energy exchange quantity and power price. With demand side management, the

CMIESs are optimized to purchase power during 4:00-7:00 to reduce power purchase costs. Also, the VPP gives a relatively low energy purchase price when CMIESs determine to sell energy to make profits during 15:00-18:00 and 24:00.

Fig. 7 illustrates the energy scheduling results of the VPP in different slots. Based on the sampled scenarios, the PV generation supplies power during 8:00 to 17:00. Thus, for a better economic benefit, the excessive PV output is sold to other participants. For the energy storage operation, the PHS is mostly scheduled to store energy when the PV output is sufficient during 9:00 to 16:00 while other times the PHS is mostly scheduled to release energy to satisfy the load and sell energy to the grid or the coal mines. Considering the energy price in Fig. 5, the energy management of the PHS is utilized flexibly for the economic welfare of the VPP. Constrained by (14b), the SOC of the PHS at 24:00 is equal to the initial value for a sustainable scheduling.

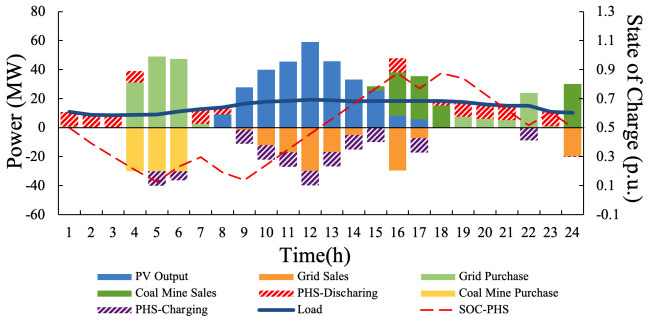

Fig. 7. The DRO energy scheduling results of the VPP.

B. Energy trading and management results of the CMIESs

With energy recovery units and coal transportation demand response, the CMIESs can optimize its energy scheduling to reduce economic cost. We take one of the CMIESs for illustration. Fig. 8 shows the optimal power dispatching results of the CMIES #1. Fig. 9 represents the energy exchange between the CMIESs and the DSO.

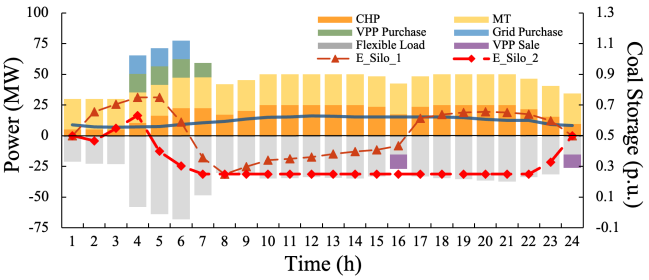

Fig. 8. Optimal Power dispatching of the CMIES #1.

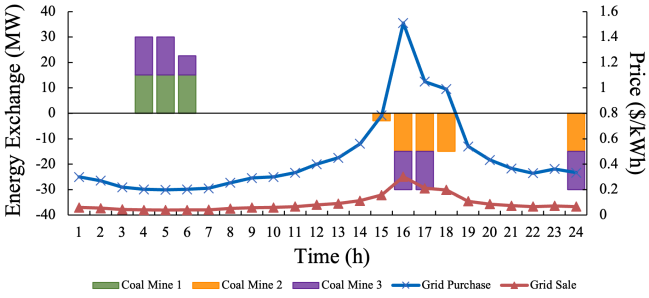

Fig. 9. Energy exchange between the CMIESs and the DSO.

From Fig. 8 and Fig. 9, the CHP and MT units are to generate power to satisfy the power demand. Considering carbon emission tax and carbon transactions, the CHPs and MTs in various CMIESs share different proportion of power supply due to their various carbon emission parameters. Besides, according to the energy price in Fig. 5, the insufficient power shortage is supplied by purchasing power from the VPP or the DSO during 4:00-7:00 while the excessive power output is sold to the VPP or the DSO to make a profit. The flexible loads, including the BCs and the heat pumps, shifted their power demand to 4:00-7:00 by shaving the demand during 15:00-18:00 and 24:00.

As the dash lines shows, the coal silos are scheduled to store and release the raw coal within the coal storage constraints, which play the role of the VES. The stored raw coal in different levels of silos increases at the beginning, which means the BCs in the workface deliver the coal out for mining safety while the upper level BCs deliver less coal for saving energy cost. When the stored raw coal decreases, the BCs in the shaft or on the ground deliver more coal out of the silos to consume more power during low price periods.

Detailed coal transportation demand response are shown in Fig. 10. The feed rate of the BC in the workface is stable and equal to the raw coal production. The BCs in other level are scheduled more flexibly as their feed rate can reach the maximal delvery capacity and also go down to the minimal limit. Hence, the BCs are scheduled to enhance the demand response for a better economic benefits when considering energy price and carbon tax.

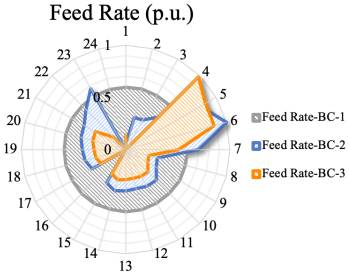

Fig. 10. Coal transportation demand response in CMIES #1.

Thermal energy dispatching balance of the CMIESs are shown in the Fig. 11. The main thermal power supply of each CMIESs are the CHPs and MTs. They are scheduled to supply thermal energy coordinated with electrical power. Thus their thermal output is coordinated with the same operational scheduling of their power dispatching respectively. Apart from the energy recovery units, the WSHPs and the ASHPs supply their maximal thermal power due to their lower maintenance cost and no carbon emission caused by fossil fuel compared with those of the CHPs and MTs. As flexible energy storage units, the TSTs are scheduled to compensate the insufficient thermal supply and store energy when the thermal output is excessive.

C. Performance Evaluation

Firstly, we discuss the privacy preserving of the ADMM-based DRO algorithm with the PoA blockchain. Fig. 12 shows the mining process of the PoA blockchain and Fig. 13

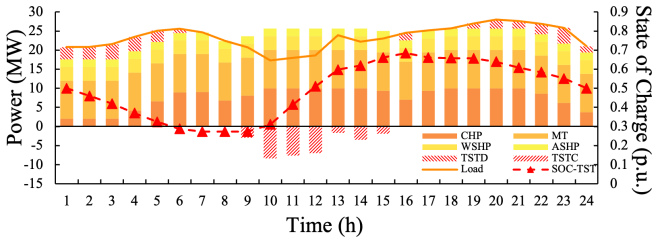

Fig. 11. Thermal energy dispatching result of the CMIES #1

represents the deployment of the smart contract in Algorithm 2. Before the convergence, the variable updating, including the x-*update*, z-*update* and u-*update* in ADMM, are addressed in the PoA blockchain. Fig. 14 shows the 2-norm residual in the Algorithm 1 and 2. It can be observed that with the variable update process in the blockchain, the residual is reduced to 10^{-12} with 10 iterations. The reduced residual reached the stopping criteria of the smart contract and satisfied the converge conditions for the ADMM-based algorithm [24]. Hence, the private information is effectively preserved with the coordination of the smart contract.

Fig. 15 shows the nodal voltage of the distribution network at each time slot. The errors are measured by the per-unit value by setting the voltage base values to 12.66 kV. The maximum and the minimum voltages are 0.902 and 1.066, respectively. The nodal voltage is acceptable in practice considering the voltage limits are 0.9-1.1 p.u., which illustrates that the proposed energy trading framework and market clearing algorithm can effectively secure the operation of the distribution network.

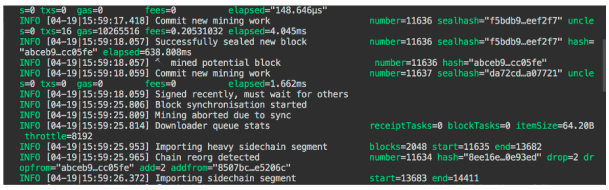

Fig. 12. The mining process of the PoA blockchain.

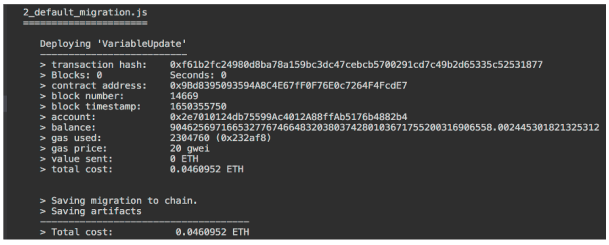

Fig. 13. The deployment of the smart contract.

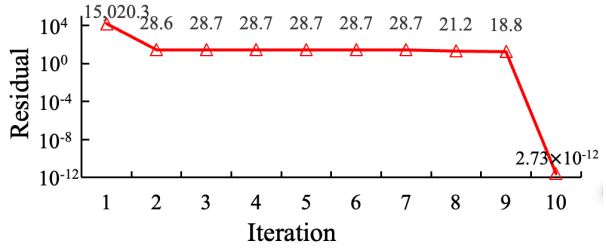

Fig. 14. Trace of the residual evaluated in the ADMM-based DRO algorithm.

To illustrate how the Stackelberg game will affect the carbon trading, we make the comparison between the carbon trading in the bi-level market and the peer-to-peer market. The regional emission caps of both market are all set to 2240 ton. In the P2P market the VPP is not engaged in

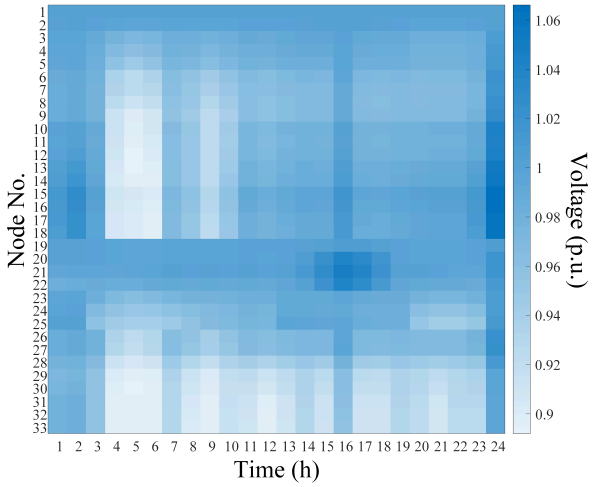

Fig. 15. Nodal voltage of the distribution network.

the carbon emission trading while in the bi-level market they can carry trades to sell the emission right to CMIESs at the purchase price and pay the emission tax price. To validate the effectiveness of the proposed method, three benchmarks are compared:

Method # 1: Deterministic optimization method: The PV output is regarded as deterministic forecasted data.

Method # 2: Two-stage RO method: The bi-level energy and carbon trading with energy management is solved by the two-stage RO method, the uncertainty degree is set to 0.2.

Method # 3: The DRO method: The bi-level problem is solved by the DRO method with 50 scenarios of the PV output. The Wasserstein distance radius is set to 0.2.

Table II shows that with the engagement of the VPP, the carbon emission cap for each CMIES is lower. In both markets, the CMIES#2 have emission right surplus as its carbon emission is within the cap limit. Thus, the CMIES#2 can sell the emission right to other CMIESs whose local emissions exceed their emission cap. Compared to the P2P market, the CMIES#2 and #3 are to purchase more carbon emission rights to ensure their own emission under the cap. For the VPP, due to its clean energy generation from PV, the VPP has no local carbon emission, which indicates that the VPP can make use of its emission allowance to trade by selling the emission right to others and paying the tax for making a profit. From the perspective of local carbon emission, in the bi-level market, the CMIESs are to schedule their own energy units to reduce local carbon emission. Thus, the regional total emission is reduced to 2142.16 ton. It can be concluded that compared to the P2P carbon market, the bi-level carbon trading contributes to 4.37% regional decarbonization.

The performance comparison results in Table III illustrates that the different optimization approach for uncertain PV output will not affect the energy trading cost of the CMIESs. As the leader of the game, VPP will only decide its pricing policy while the energy exchange quantity is decided by the CMIESs. When the VPP is to maximize the power purchase price for profits, it is equal for the CMIESs to choose purchase power from the VPP or from the DSO. Thus, uncertainties from the PV will not affect the energy transaction between the VPP and the CMIES. However, the uncertain PV output

TABLE II
PERFORMANCE COMPARISON ON OPTIMIZATION METHODS

	P2P carbon market				Bi-level carbon market			
Participants	CMIES #1	CMIES #2	CMIES #3	VPP	CMIES #1	CMIES #2	CMIES #3	VPP
Local Carbon Emission (ton)	839.75	620.29	779.97	-	837.76	545.64	758.77	0
Emission Right Trading (ton)	93.07	-126.38	33.30	-	277.76	-14.36	198.77	-462.16
Emission Cap (ton)	746.67	746.67	746.67	-	560.00	560.00	560.00	560.00
Regional Emission/Cap (ton)	2240/2240				2142.16/2240			

TABLE III
COMPARISON BETWEEN BI-LEVEL CARBON MARKET AND P2P CARBON MARKET

Result	**Method #1**		**Method #2**		**Method #3**	
	VPP	CMIESs	VPP	CMIESs	VPP	CMIESs
Trading cost with DSO ($)	-1082.88	-4453.46	7733.82	-4453.46	5114.02	-4453.46
Trading cost between the VPP and CMIESs ($)	-24124.75	24124.75	-24124.75	24124.75	-24124.75	24124.75
Total cost ($)	-25691.54	7569.73	-16874.76	7569.73	-19495.56	7569.73
Regional welfare ($)	-18121.81		-9305.03		-11924.83	

will affect the energy trading between the VPP and the DSO. For **Method #1**, the VPP makes a profit of $1082.88 by selling excessive PV generation to the DSO. This is due to the lack of consideration of uncertainties. The deterministic case has no robustness in optimization. Hence, for application, its optimal solution cannot reflect the reality of uncertain PV output. For **Method #2**, the trading cost between the VPP and the DSO is $7733.82, which is conservative by finding the worst case in the RO uncertainty set. Meanwhile, that trading cost with DSO in **Method #3** is $5114.02, which can overcome the conservation of the RO method and reflect the uncertain PV output in real cases. Correspondingly, the regional welfares, the total cost of all the VPP and the CMIESs, will be affected by the way to deal with PV output, which are -$18121.81, -$9305.03 and -$11924.83. Hence, the solution with ADMM-based DRO will provide a comparatively robust but also not too optimistic energy trading cost.

VI. CONCLUSION

In this paper, a Stackelberg game based bi-level trading framework with energy management is proposed to deal with carbon and energy integrated energy trading in coal mines. The uniqueness and existence of the Stackelberg game equilibrium of the proposed model is proved. To deal with uncertainties from the PV output, the energy management of the VPP is solved by the DRO method using the Wasserstein ambiguity set. Considering the security of private trading information, the ADMM-based DRO algorithm is proposed to address the trading problem in a distributed manner. Further, a Proof of Authority (PoA) blockchain enabled market platform is developed for a safe and anonymous transaction environment. Numerical cases are simulated to validate the effectiveness of the proposed method. Results indicate that the proposed bi-level carbon and energy market can contribute towards regional decarbonization. Also, the proposed ADMM-based DRO can effectively protect private information by the PoA blockchain. Compared with traditional methods, the proposed ADMM-based DRO algorithm immune to various uncertainties from the PV output and overcomes the conservatism of the robust optimization method.

For future work, firstly the coordination between the day-ahead market and the real-time market can be investigated under the joint carbon and energy trading framework. Secondly, considering ancillary services products, the price adjustment mechanism can be introduced into the energy market.

REFERENCES

[1] I. Karakurt *et al.*, "Mine ventilation air methane as a sustainable energy source," *Renewable and Sustainable Energy Reviews*, vol. 15, no. 2, pp. 1042–1049, 2011.
[2] Q. Zhang *et al.*, "Coal mine gas separation of methane via clathrate hydrate process aided by tetrahydrofuran and amino acids," *Applied Energy*, vol. 287, p. 116576, 2021.
[3] Al-Habaibeh *et al.*, "Performance analysis of using mine water from an abandoned coal mine for heating of buildings using an open loop based single shaft gshp system," *Applied Energy*, vol. 211, pp. 393–402, 2018.
[4] H. Huang *et al.*, "Two-stage robust stochastic scheduling for energy recovery in coal mine integrated energy system," *Applied Energy*, vol. 290, p. 116759, 2021.
[5] Y. Mu *et al.*, "Optimal scheduling method for belt conveyor system in coal mine considering silo virtual energy storage," *Applied Energy*, vol. 275, p. 115368, 2020.
[6] H. Hu *et al.*, "Enhanced evolutionary multi-objective optimization-based dispatch of coal mine integrated energy system with flexible load," *Applied Energy*, vol. 307, p. 118130, 2022.
[7] J. Fan *et al.*, "Preliminary feasibility analysis of a hybrid pumped-hydro energy storage system using abandoned coal mine goafs," *Applied Energy*, vol. 258, p. 114007, 2020.
[8] R. Gao *et al.*, "Optimal dispatching of wind-pv-mine pumped storage power station: A case study in lingxin coal mine in ningxia province, china," *Energy*, vol. 243, p. 123061, 2022.
[9] Z. Yi *et al.*, "Bi-level programming for optimal operation of an active distribution network with multiple virtual power plants," *IEEE Transactions on Sustainable Energy*, vol. 11, no. 4, pp. 2855–2869, 2020.
[10] National Bureau of Statics, *Stastical year book of China*. Beijing: China statics Press, 2020.
[11] Y. Liu *et al.*, "Gaussian process-based approach for bilevel optimization in the power system – a critical load restoration case," *arXiv preprint arXiv:2012.01388v2*, 2022.
[12] P. Parikshit *et al.*, "Optimal steady-state voltage control using gaussian process learning," *IEEE Transactions on Industrial Informatics*, vol. 17, no. 10, pp. 7017–7027, 2020.
[13] L. P. M. I. Sampath *et al.*, "Peer-to-peer energy trading enabled optimal decentralized operation of smart distribution grids," *IEEE Transactions on Smart Grid*, vol. 13, no. 1, pp. 654–666, 2022.
[14] Azim *et al.*, "Coalition graph game-based p2p energy trading with local voltage management," *IEEE Transactions on Smart Grid*, vol. 12, no. 5, pp. 4389–4402, 2021.
[15] W. Zhong *et al.*, "Cooperative p2p energy trading in active distribution networks: An milp-based nash bargaining solution," *IEEE Transactions on Smart Grid*, vol. 12, no. 2, pp. 1264–1276, 2021.
[16] L. Wang *et al.*, "Non-cooperative game-based multilateral contract transactions in power-heating integrated systems," *Applied Energy*, vol. 268, p. 114930, 2020.
[17] Mediwaththe *et al.*, "Competitive energy trading framework for demand-side management in neighborhood area networks," *IEEE Transactions on Smart Grid*, vol. 9, no. 5, pp. 4313–4322, 2018.

[18] N. Liu *et al.*, "Energy sharing management for microgrids with pv prosumers: A stackelberg game approach," *IEEE Transactions on Industrial Informatics*, vol. 13, no. 3, pp. 1088–1098, 2017.
[19] L. He *et al.*, "An occupancy-informed customized price design for consumers: A stackelberg game approach," *IEEE Transactions on Smart Grid*, 2022.
[20] N. Liu *et al.*, "Energy-sharing provider for pv prosumer clusters: A hybrid approach using stochastic programming and stackelberg game," *IEEE Transactions on Industrial Electronics*, vol. 65, no. 8, pp. 6740–6750, 2018.
[21] Nezamabadi *et al.*, "Arbitrage strategy of renewable-based microgrids via peer-to-peer energy-trading," *IEEE Transactions on Sustainable Energy*, vol. 12, no. 2, pp. 1372–1382, 2021.
[22] X. Zhou *et al.*, "Partial carbon permits allocation of potential emission trading scheme in australian electricity market," *IEEE Transactions on Power Systems*, vol. 25, no. 1, pp. 543–553, 2009.
[23] K. Zhang *et al.*, "A framework for multi-regional real-time pricing in distribution grids," *IEEE Transactions on Smart Grid*, vol. 10, no. 6, pp. 6826–6838, 2019.
[24] S. Boyd *et al.*, "Distributed optimization and statistical learning via the alternating direction method of multipliers," *Foundations and Trends® in Machine learning*, vol. 3, no. 1, pp. 1–122, 2011.
[25] Haggi *et al.*, "Multi-round double auction-enabled peer-to-peer energy exchange in active distribution networks," *IEEE Transactions on Smart Grid*, vol. 12, no. 5, pp. 4403–4414, 2021.
[26] Ullah *et al.*, "Peer-to-peer energy trading in transactive markets considering physical network constraints," *IEEE Transactions on Smart Grid*, vol. 12, no. 4, pp. 3390–3403, 2021.
[27] J. Kang, R. Yu, X. Huang, S. Maharjan, Y. Zhang, and E. Hossain, "Enabling localized peer-to-peer electricity trading among plug-in hybrid electric vehicles using consortium blockchains," *IEEE Transactions on Industrial Informatics*, vol. 13, no. 6, pp. 3154–3164, 2017.
[28] J. Yang, J. Dai, H. B. Gooi, H. D. Nguyen, and P. Wang, "Hierarchical blockchain design for distributed control and energy trading within microgrids," *IEEE Transactions on Smart Grid*, vol. 13, no. 4, pp. 3133–3144, 2022.
[29] K. Gai, Y. Wu, L. Zhu, M. Qiu, and M. Shen, "Privacy-preserving energy trading using consortium blockchain in smart grid," *IEEE Transactions on Industrial Informatics*, vol. 15, no. 6, pp. 3548–3558, 2019.
[30] M. Yan, M. Shahidehpour, A. Alabdulwahab, A. Abusorrah, N. Gurung, H. Zheng, O. Ogunnubi, A. Vukojevic, and E. A. Paaso, "Blockchain for transacting energy and carbon allowance in networked microgrids," *IEEE Transactions on Smart Grid*, vol. 12, no. 6, pp. 4702–4714, 2021.
[31] Y. Jiang, K. Zhou, X. Lu, and S. Yang, "Electricity trading pricing among prosumers with game theory-based model in energy blockchain environment," *Applied Energy*, vol. 271, p. 115239, 2020.
[32] N. Liu, L. Tan, L. Zhou, and Q. Chen, "Multi-party energy management of energy hub: A hybrid approach with stackelberg game and blockchain," *Journal of Modern Power Systems and Clean Energy*, vol. 8, no. 5, pp. 919–928, 2020.
[33] Q. Yang and H. Wang, "Blockchain-empowered socially optimal transactive energy system: Framework and implementation," *IEEE Transactions on Industrial Informatics*, vol. 17, no. 5, pp. 3122–3132, 2021.
[34] A. Esmat, M. de Vos, Y. Ghiassi-Farrokhfal, P. Palensky, and D. Epema, "A novel decentralized platform for peer-to-peer energy trading market with blockchain technology," *Applied Energy*, vol. 282, p. 116123, 2021.
[35] H. Ruan, H. Gao, H. Qiu, H. B. Gooi, and J. Liu, "Distributed operation optimization of active distribution network with p2p electricity trading in blockchain environment," *Applied Energy*, vol. 331, p. 120405, 2023.
[36] Z. Li *et al.*, "A risk-averse adaptively stochastic optimization method for multi-energy ship operation under diverse uncertainties," *IEEE Transactions on Power Systems*, vol. 36, no. 3, pp. 2149–2161, 2021.
[37] S. Zhang *et al.*, "Modeling and energy efficiency optimization of belt conveyors," *Applied Energy*, vol. 88, no. 9, pp. 3061–3071, 2011.
[38] R. Zhu, H. Wei, and X. Bai, "Wasserstein metric based distributionally robust approximate framework for unit commitment," *IEEE Transactions on Power Systems*, vol. 34, no. 4, pp. 2991–3001, 2019.
[39] P. Xiong, P. Jirutitijaroen, and C. Singh, "A distributionally robust optimization model for unit commitment considering uncertain wind power generation," *IEEE Transactions on Power Systems*, vol. 32, no. 1, pp. 39–49, 2017.
[40] Gurobi Optimization, LLC, "Gurobi Optimizer Reference Manual," 2021. [Online]. Available: https://www.gurobi.com